

# Ubiquity of metastable-to-stable crossover in weakly chaotic dynamical systems

Fulvio Baldovin<sup>a</sup>, Luis G. Moyano<sup>a</sup>, Ana P. Majtey<sup>b</sup>,  
Alberto Robledo<sup>c</sup> and Constantino Tsallis<sup>a</sup>

<sup>a</sup>*Centro Brasileiro de Pesquisas Físicas,  
Rua Xavier Sigaud 150, 22290-180 Rio de Janeiro – RJ, Brazil*

<sup>b</sup>*Facultad de Matemática, Astronomía y Física, Universidad Nacional de Córdoba,  
Ciudad Universitaria, 5000, Córdoba, Argentina*

<sup>c</sup>*Instituto de Física, Universidad Nacional Autónoma de México,  
Apartado Postal 20-364, México 01000 D.F., Mexico*

---

## Abstract

We present a comparative study of several dynamical systems of increasing complexity, namely, the logistic map with additive noise, one, two and many globally-coupled standard maps, and the Hamiltonian Mean Field model (i.e., the classical inertial infinitely-ranged ferromagnetically coupled XY spin model). We emphasize the appearance, in all of these systems, of metastable states and their ultimate crossover to the equilibrium state. We comment on the underlying mechanisms responsible for these phenomena (weak chaos) and compare common characteristics. We point out that this ubiquitous behavior appears to be associated to the features of the nonextensive generalization of the Boltzmann-Gibbs statistical mechanics.

*Key words:* Nonlinear dynamics, Statistical mechanics, Metastable (quasistationary) states

*PACS:* 05.20.-y, 05.45.-a, 05.70.Ln, 05.90.+m

---



---

*Email addresses:* baldovin@cbpf.br (Fulvio Baldovin), moyano@cbpf.br (Luis G. Moyano), amajtey@famaf.unc.edu.ar (Ana P. Majtey), robledo@fisica.unam.mx (Alberto Robledo), tsallis@cbpf.br (Constantino Tsallis).

## 1 Introduction

The statistical-mechanical comprehension of the occurrence and eventual disappearance of out-of-equilibrium quasistationary states (QSS), referred here also as metastable states, is an important undertaking that nowadays attracts the attention of researchers in various fields, ranging from weakly chaotic nonlinear dynamics to slow glassy dynamics in condensed matter. Under specific classes of initial conditions, the dynamics in these systems displays two-step relaxation processes, entering first one or more periods of little variation before a crossover to the final equilibrium state. The QSS are conjectured to emerge as the result of long-ranged correlations or interactions amongst the elements of the system or long-ranged time correlations in the orbits of iterated maps. An interesting statistical-mechanical model that displays QSS is the Hamiltonian Mean Field (HMF) model [1], that in its simplest version consists of a set of  $N$  inertial XY classical spins or rotors all of which interact equally with each other. But also, interestingly, the most relevant features of QSS dynamics are displayed by considerably simpler nonlinear dynamical maps, as it is the case of conservative coupled maps [2] and also by single, dissipative, one-dimensional maps, like the prototypical logistic map close to the edge of chaos and in the presence of external noise [3].

In this paper we present a comparative study of the aforementioned models, starting our discussion with low-dimensional nonlinear maps and ending it with the HMF model. We emphasize the analogies found between their dynamical properties and indicate the mechanisms that give raise to the QSS as well as those responsible for the crossover to the equilibrium state. In all of these cases the quantities that describe dynamical evolution seem to be associated to the predictions of the nonextensive generalization [4] of the Boltzmann-Gibbs (BG) statistical mechanics. Also, in all of these examples there is clear evidence of the non-commutability of the infinite time limit with other important parameter limits, such as the thermodynamic limit ( $N \rightarrow \infty$ ) or the limit of vanishing noise amplitude. Moreover, there is a common indication that, in the characterization of the phase space available for dynamical evolution, there appears evidence of fractalization and of ergodicity failure.

The paper is organized as follows. In the next section we describe how the dynamics at the edge of chaos of the logistic map leads, via the addition of external noise, to the crossover from QSSs to a strongly chaotic state that is the analog of the BG equilibrium state [3]. We present here new numerical evidence by means of an ensemble implementation of the dynamics in this system. In section 3 we note that the emergence of QSSs and eventual departure from them appear associated to the complex structure of phase space accessibility in symplectic maps governed by the Kolmogorov-Arnold-Moser (KAM) theorem [2]. We also show new results that indicate that the QSS, present at

the lowest possible dimensions, persists as hundreds of symplectic maps are (globally) coupled. Section 4 is devoted to the QSS of the HMF model. Particular attention is paid to the time evolution of the anomalous probability distribution functions (PDFs) for the velocities, and also to basic questions referring to the measurability of temperature and to the zeroth principle of thermodynamics as it relates to the QSS [5]. Finally, in section 5 we draw our conclusions, we make reference to the existing analogies amongst the different models described and discuss the underlying mechanism that gives raise to the QSS.

## 2 QSS in the logistic map with external noise

Let us start our analysis by recalling [3] that phenomena like two-step relaxation and aging can be displayed at the lowest possible dimension, namely, by means of a one-dimensional map. For this purpose we consider the paradigmatic logistic map with additive white noise,

$$x_{\tau+1} = 1 - \mu x_{\tau}^2 + \xi_{\tau}\sigma, \quad \tau = 0, 1, \dots, \quad x \in [-1, 1], \quad \mu \in [0, 2], \quad (1)$$

where  $\xi_{\tau}$  is Gaussian-distributed and delta-correlated,  $\langle \xi_{\tau} \rangle_{\xi} = 0$ ,  $\langle \xi_{\tau} \xi_{\tau'} \rangle_{\xi} = \delta_{\tau\tau'}$ , and  $\sigma$  measures the noise intensity. As it is well known, for  $\sigma = 0$  the Feigenbaum attractor at the edge of chaos  $\mu = \mu_c \equiv 1.401155189\dots$  is the accumulation point of both the period-doubling and band-splitting cascades. The Lyapunov coefficient is zero [6] and the attractor is a cantor set of fractal dimension  $d_f = 0.5338\dots$ . It has been analytically proved by means of the conventional renormalization-group approach for this type of map that the dynamics at this critical point is unmistakably associated to the nonextensive statistical mechanics [7]. Specifically, the sensitivity to initial conditions is actually given in a closed form by a  $q$ -exponential function and it is related to the rate of entropy production via a  $q$ -generalized Pesin identity, linking the sensitivity to initial conditions to the nonextensive expression for the entropy,  $S_q = \ln_q W$  (where  $W$  is the number of equally-probable positions of an ensemble of iterates at a given time). For this stationary state the index  $q$  takes the specific value  $q = 0.2445\dots$ . Let us remind the reader that the  $q$ -exponential and its inverse the  $q$ -logarithm are defined, respectively, as  $\exp_q(x) \equiv [1 + (1 - q)x]^{1/(1-q)}$  and  $\ln_q(x) \equiv (x^{1-q} - 1)/(1 - q)$ , and that these expressions reduce to the usual exponential and logarithmic functions in the limit  $q \rightarrow 1$ .

More precisely, the Feigenbaum attractor can be described by means of a set of position subsequences generated when the iterative map is given the initial position  $x_0 = 0$  [7]. See the empty circles in Fig. 1(a) where we have plotted the absolute value of these positions  $|x_{\tau}|$  and time  $\tau$  at which they are reached

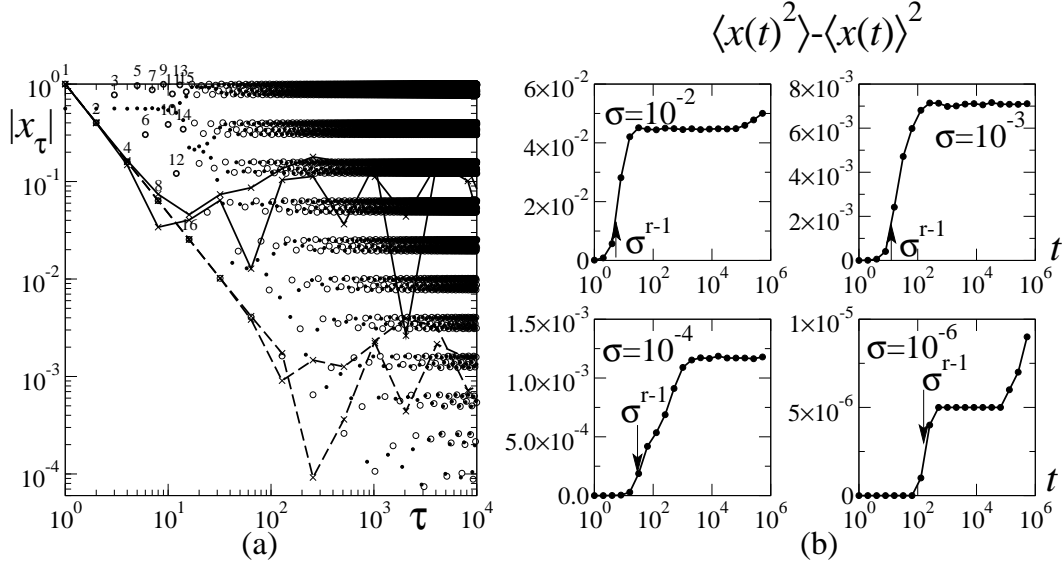


Fig. 1. (a) Phase space structure of the logistic map with and without additive noise. Empty circles correspond to the attractor at  $\mu = \mu_c$  and  $\sigma = 0$ , obtained by iterating  $x_0 = 0$  (the numbers label time  $\tau = 1, \dots, 16$ ). Small dots correspond to  $x_0 = 0.56023$ , close to a repeller, the unstable solution of  $x = 1 - \mu_c x^2$ . Full (and dashed) lines represent two trajectories for  $\mu = \mu_c$ ,  $\sigma = 10^{-3}$  (and  $\sigma = 10^{-6}$ ). (b) Plateaux structure. Time evolution (using the shifted time  $t = 2^n - 1$ ) of the variance of an ensemble of  $M = 10^4$  trajectories all starting at  $x_0 = 0$ , for different orders of magnitude of the noise strength  $\sigma$ . Notice that the crossover times coincide with  $\sigma^{r-1}$  (with  $r \simeq 0.633$ ) indicated with arrows (see text).

in logarithmic scales. Each of the subsequences is labelled by an integer  $k = 0, 1, \dots$  and each is generated by the time subsequence  $\tau_k = (2k + 1)2^{n-k}$ , with  $n = 0, 1, \dots$  and  $n \geq k$ . This can be appreciated in Fig. 1(a). In the following we will focus on the principal subsequence  $\tau_0 = 2^n$ . Another important feature of Fig. 1(a) is that the logarithm of the attractor positions appear clearly divided into an infinite number of equally-spaced horizontal bands. In the empty space between any two bands there are points called *repellers*, the unstable solutions of the iterated equation  $x = 1 - \mu_c x^2$ . (See the small dots in Fig. 1(a)). At the chaos threshold of the logistic map with  $\sigma \neq 0$  the dynamics is governed by two competing phenomena: On the one hand the action of the noise is to drive the iterates out of the bands, and on the other hand the instability in the neighborhood of the repellers sends the positions back into the attractor bands. When the noise intensity is large enough to fill a gap between bands, the result is that the iterates are able to jump from one band to the next. (See full and dashed lines in Fig. 1(a)). Since the band gaps in  $|x|$ -space are of variable size, increasing in size as  $|x| \rightarrow 1$ , the motion becomes confined among some few bands for a certain amount of time but at longer times the iterates are able to spread to other more distant bands.

The analysis of the crossover time  $t_c$  for the broadening of the attractor bands produced by the noise can be made quantitative. At the edge of chaos  $\mu = \mu_c$ , for  $\sigma \neq 0$ , the iterated position of  $x_0 = 0$  at shifted time  $t = \tau_0 - 1$  is given by (see [3] for details):

$$x_t = \exp_{2-q}(-\lambda_q t)[1 + \xi_t \sigma \exp_r(\lambda_r t)], \quad (2)$$

where  $q = 1 - \ln 2 / \ln \alpha = 0.2445\dots$ ,  $\lambda_q = \ln \alpha / \ln 2 = 1.3236\dots$  is the generalized Lyapunov coefficient,  $r = 1 - \ln 2 / \ln \kappa \simeq 0.633$ ,  $\lambda_r = \ln \kappa / \ln 2 \simeq 2.727$  ( $\alpha = 2.50290\dots$  being one of Feigenbaum's universal constants and  $\kappa \simeq 6.619$  a constant associated to the noise term). Let us consider now a different trajectory  $x'_t$  also starting at the origin at  $t = 0$ ,  $x'_0 = 0$ . Since the noise acts independently on each trajectory, after time  $t$  the orbit's separation is given by

$$x_t - x'_t = \exp_{2-q}(-\lambda_q t) \exp_r(\lambda_r t) \sigma (\xi_t - \xi'_t). \quad (3)$$

At time  $t = 2^n - 1$  the separation between bands at which the iterate is located is of order  $\exp_{2-q}(-\lambda_q t)$ . Using  $\xi_t - \xi'_t \sim 1$  we obtain an estimate of the crossover time  $t_c$  at which the noise-assisted jumps into different bands starts to take place. This is

$$\exp_r(\lambda_r t_c) \sigma \sim 1 \Rightarrow t_c \sim \sigma^{r-1}. \quad (4)$$

In order to display the many-plateaux structure of time evolution in this dynamical model we consider next an ensemble of  $M = 10^3$  independent copies of the map (1) at the edge of chaos  $\mu = \mu_c$ . The initial positions are  $x_0 = 0 \forall M$  and we measure the variance  $\langle x_t^2 \rangle - \langle x_t \rangle^2$  (which plays a role analogous to the *temperature* in the statistical-mechanical description of Hamiltonian systems) of the distribution of positions at time  $t = 2^n - 1$ . Fig. 1(b) shows a numerical corroboration of previous results [3], for different values of the noise intensity  $\sigma$ . While in the first plateau the variance is zero, as the dynamics of all  $M$  trajectories is confined to the attractor, at the crossover time  $t_c \sim \sigma^{r-1}$  the ensemble of orbits starts spreading and the variance increases until a second plateau is reached where it saturates as a consequence of the confinement induced by the unstable repeller regions. As it can be well appreciated in Fig. 2, for long enough times it is possible to see another increment of the variance as the iterates are able to reach other bands of the attractor. The whole process ends when all bands become occupied and the variance is consequently of order 1.

A two-step process of relaxation is known to be one of the main dynamical properties displayed by supercooled liquids close to glass formation [8]. Two other characteristic features of glassy dynamics are the so-called Adam-Gibbs formula and the scaling property known as aging. The first is a relation between the relaxation time  $t_c$  (e.g. the viscosity or the inverse of the diffusivity) and the entropy  $S_{conf}$  associated to the number of possible molecular minimum

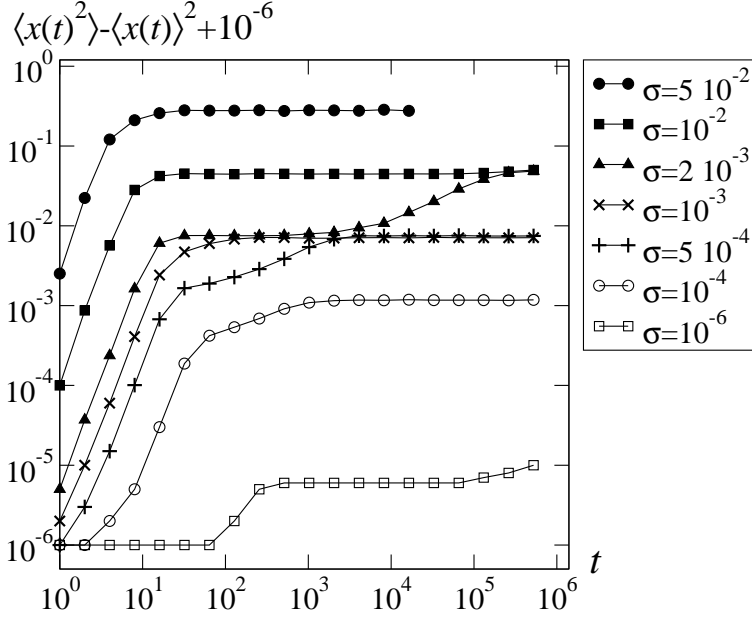


Fig. 2. Plateaux structure for the logistic map with additive noise. Time evolution (using  $t = 2^n - 1$ ) of the variance of an ensemble of  $M = 10^4$  trajectories all starting at  $x_0 = 0$ , for different values the noise strength  $\sigma$ . In order to display data with different orders of magnitude, the  $y$ -axis has been plotted in a logarithmic scale with a shift of  $10^6$ .

energy configurations in the fluid [8]. The second is the loss of time translation invariance, named aging [9], that is due to the fact that properties of glasses depend on the procedure by which they are obtained. The time decrease of relaxation functions and correlations exhibit a scaling dependence on the ratio  $t/t_w$  where  $t_w$  is a waiting time. As the counterpart to the Adam-Gibbs formula, it has recently been shown [3] that the logistic map at  $\mu_c$  for  $\sigma \neq 0$  presents a relationship between the plateau duration  $t_c$ , and the entropy  $S_{conf}$  for the state that comprises the largest number of (iterate positions) bands allowed by noise intensity. This entropy is obtained from the probability of chaotic band occupancy at position  $x$  [3]. Also, the trajectories at  $\mu_c$  in the limit  $\sigma \rightarrow 0$  have been shown [3] to obey a scaling property characteristic of aging, of the form  $x_{t+t_w} = g^{(t_w)}(0) \exp_q(-\lambda_q t/t_w)$  where  $g^{(t_w)}(0)$  is the  $t_w$ -times composition of the Feigenbaum fixed-point map function  $g(0)$ .

### 3 QSS in coupled symplectic maps

Symplectic maps are important tools in the study of Hamiltonian systems. If we consider a *time-independent* Hamiltonian system with  $n$  degrees of freedom ( $2n$ -dimensional Gibbs  $\Gamma$ -space), a  $(2n - 2)$ -dimensional symplectic map is the result of taking a Poincaré section over the constant energy hypersurface [10]. The recurrence time is discrete and the map is useful in displaying the

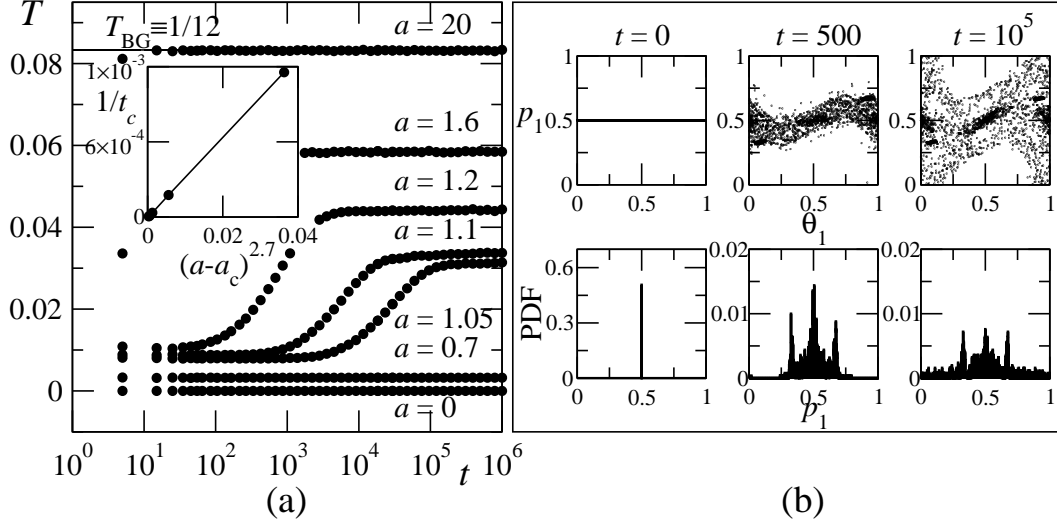


Fig. 3. QSS in the standard map (i.e.,  $N = 1$ ). (a)  $T(t)$  for typical values of  $a$ . We start with “water bag” initial conditions ( $M = 2500$  points in  $0 \leq \theta_1 \leq 1$ ,  $p_1 = 0.5 \pm 5 \cdot 10^{-4}$ ). Inset: Inverse crossover time  $t_c$  (inflection point between the QSS and the BG regimes with the time axis plotted in logarithmic scale) vs.  $1/(a_1 - a_c)^{2.7}$ . (b) Time evolution of the ensemble in (a) for  $a_1 = 1.1$  (first row) and PDF of its angular momentum (second row).  $t = 0$ : Initial conditions;  $t = t_1 = 500$ : The ensemble is mostly restricted by cantori;  $t = t_2 = 10^5$ : The ensemble is confined by KAM-tori. See [2] for further details.

stationary, recurrent properties of the original Hamiltonian system. Interestingly enough, a  $2n$ -dimensional symplectic map is also the result of a Poincaré section in the phase space of a *time-dependent* Hamiltonian system with  $n$  degrees of freedom ( $2n + 1$  dimensions), with a periodic dependence on time [10]. As a consequence of the symplectic structure, the Lyapunov spectra in the  $d$ -dimensional phase space of the map ( $d$  being an even number) is characterized by  $d/2$  pairs of Lyapunov coefficients, where each element of the pair is the negative of the other.

A prototypical 2-dimensional symplectic map, that displays the KAM mechanism for the transition from regularity to chaos, is the Chirikov-Taylor *standard map* (see, e.g., [10] and references therein). Since fundamental dynamical processes, like for example Arnold diffusion, occur only for  $d > 2$ , it is interesting to consider more generally the case of  $N$  *symplectic* and *globally* coupled standard maps ( $d = 2N$ ), described, for example, by the equations:

$$\begin{aligned} \theta_i(t+1) &= p_i(t+1) + \theta_i(t) + \frac{b}{N-1} \sum_{\substack{m=1 \\ m \neq i}}^N p_m(t+1) \pmod{1}, \\ p_i(t+1) &= p_i(t) + \frac{a}{2\pi} \sin[2\pi\theta_i(t)] \pmod{1}, \end{aligned} \quad (5)$$

where  $t = 1, 2, \dots$ ,  $i = 1, 2, \dots, N$ ,  $b \in \mathbb{R}$  is the coupling constant (in the

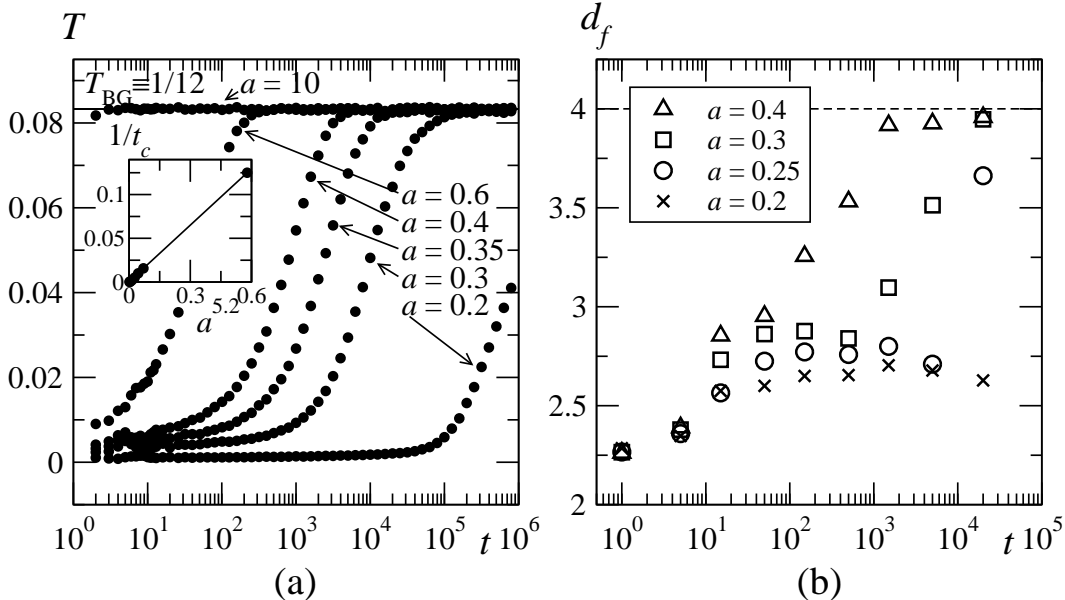


Fig. 4. QSS in two coupled standard maps (i.e.,  $N = 2$ ). (a)  $T(t)$  for  $b = 2$  and typical values of  $a$ . We start with “water bag” initial conditions ( $M = 1296$  points with  $0 \leq \theta_1, \theta_2 \leq 1$ , and  $p_1, p_2 = 0.25 \pm 5 \cdot 10^{-3}$ ). Inset: Inverse crossover time  $t_c$  vs.  $1/a^{5.2}$ . (b) Time evolution of the fractal dimension of a single initial ensemble in the same setup of (a). See [2] for further details.

following we will fix  $b = 2$ ), and  $a \in \mathbb{R}$  is a parameter that we will use to control chaoticity;  $\theta_i$  may be regarded as an angular variable and  $p_i$  as an angular momentum (defined on a compact set though). Notice that in order to describe a system with a phase space of finite size we are considering, as usual, the map on the torus (mod 1). This map is typically chaotic for large values of  $|a|$ , while for small  $|a| \neq 0$  a complex phase-space structure develops of regular regions surrounded by a stochastic web. The stochastic web is connected for  $d > 2$  (i.e.,  $N > 1$ ) and disconnected for the marginal case  $d = 2$  (i.e.,  $N = 1$ ) (see, e.g., [11]). Intentionally we introduced a global coupling among the  $N$  standard maps: to obtain time evolution properties similar to those of the long-ranged interaction many-body Hamiltonian that we shall discuss below.

Our coupled maps display a two-plateau structure with striking analogies with both the one-dimensional map discussed in Section 2 and with the HMF model that we analyze in section 4. As in the previous section, we start by considering an ensemble of  $M$  independent copies of map (5). In trying to deduce statistical properties directly from the dynamical behavior of a Hamiltonian system – with diagonal kinetic matrix and zero average momentum – it is common practice to identify the temperature with the average squared momentum per particle (see, e.g., [12]). Because we study here situations with nonzero “bulk” motion, a natural measure of temperature is given by the variance of the total



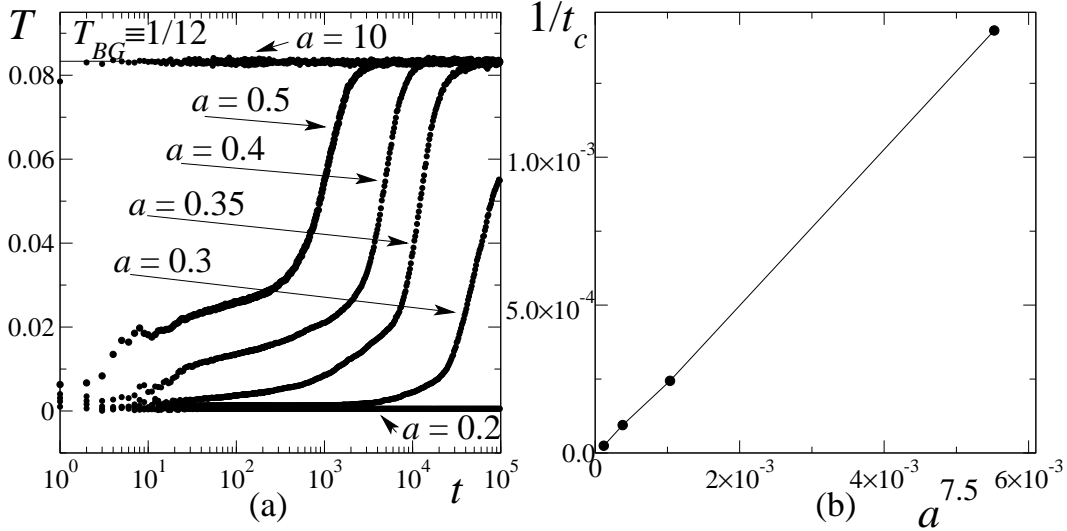


Fig. 5. QSS in  $N = 100$  coupled standard maps. (a)  $T(t)$  for  $b = 2$  and typical values of  $a$ . We start with “water bag” initial conditions ( $M = 500$  points with  $0 \leq \theta_i \leq 1$  and  $p_i = 0.25 \pm 5 \cdot 10^{-3} \forall i = 1, 2, \dots, N$ ). (b) Inverse crossover time  $t_c$  vs.  $1/a^{7.5}$ .

angular momentum,

$$T(t) \equiv \frac{1}{N} \sum_{i=1}^N \left( \langle p_i^2(t) \rangle - \langle p_i(t) \rangle^2 \right), \quad (6)$$

where  $\langle \rangle$  means ensemble average. As the classical microcanonical ensemble is based on the equal a priori probability postulate, we will call *BG temperature* the temperature associated to the uniform distribution in phase space:

$$T_{BG} \equiv \frac{1}{N} \sum_{i=1}^N \left[ \int_0^1 dp_i p_i^2 - \left( \int_0^1 dp_i p_i \right)^2 \right] = 1/12 \simeq 0.083 \quad (\forall N). \quad (7)$$

Of course, if the system is sufficiently chaotic or if the initial ensemble is sufficiently close to equilibrium (i.e., to the uniform distribution) the temperature (6) rapidly relaxes to  $T_{BG}$  as a function of the iteration time. Nevertheless, if the phase space presents complex structures *and* the initial ensemble is very far-from-equilibrium, partial barriers (see, e.g., [13]) may confine the ensemble in some limited region for quite long times, before allowing for a larger occupation of phase space. Consequently, it appears a plateau with  $T = T_{QSS} \neq T_{BG}$ .

In close analogy with the case of section 4, for our out-of-equilibrium initial conditions we set all momenta  $p_i$  randomly distributed inside a properly chosen small interval of phase space (the so-called “water bag” initial conditions), while the angles  $\theta_i$  are distributed at random inside the whole interval  $[0, 1]$ . Fig. 3(a) displays the case of a single standard map ( $N = 1$ ). For this marginal case the formation of total barriers for  $a \leq a_c = 0.971635406\dots$  prevent the formation of a second plateau below this critical point. We also notice that unless  $a$  is large enough, the temperature associated to the second plateau is

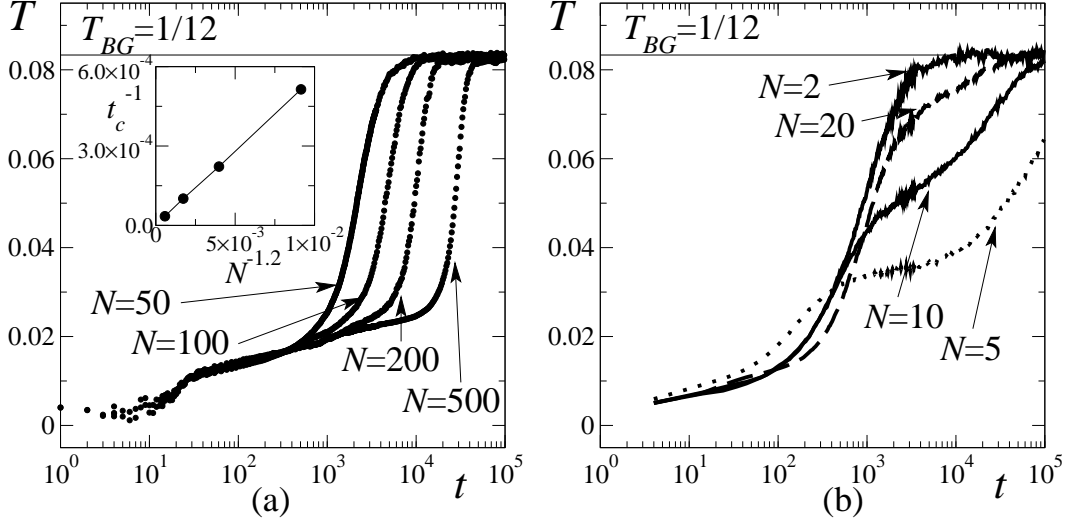


Fig. 6. Scaling of the crossover time with the number of coupled standard maps. Initial data are defined as in Fig. 5. (a)  $T(t)$  for  $a = 0.4$ ,  $b = 2$  and large values of  $N$ . Inset: Inverse crossover time  $t_c$  vs.  $1/N^{1.2}$ . (b)  $T(t)$  for  $a = 0.4$ ,  $b = 2$  and small values of  $N$ .

smaller than  $T_{BG}$ . However, the 2-dimensional case is very useful for visualizing the mechanism for plateau formation (see Fig. 3(b)). Fig. 4(a) indicates that in  $d = 4$  the topology of phase space differs from  $d = 2$ . Now total barriers for diffusive processes do not exist, and it is possible to have out-of-equilibrium initial data that leads to a dynamics with a  $T_{QQS}$  temperature two-plateau of long duration before a crossover to  $T_{BG}$ . Interestingly enough, during the first plateau the geometry of the ensemble is characterized by a nontrivial fractal dimension ( $d_f \simeq 2.7 < 4 = d$ ) that at equilibrium crosses over to the dimension of the whole phase space (see Fig. 4(b)). As shown by the new results presented in Fig. 5(a) for the 200-dimensional phase space obtained by coupling  $N = 100$  standard maps, the familiar two-plateau structure persists for large values of  $N$ . Preliminary results suggest that even for large values of  $N$  a first plateau develops with  $d_f/d < 1$ . This fact strongly reinforces the picture that there are nonzero-measure sets of initial conditions such that the system is maintained dynamically in a subset of the whole phase space, and only later occupies the entire allowed space, and adopts a BG-like statistics. This behavior is the more pronounced the closer to zero is the largest Lyapunov exponent.

It is important to stress that in all these cases the crossover time to BG statistics diverges as  $a \rightarrow 0$  (or as  $a \rightarrow a_c$  for  $d = 2$ ), as it is shown in Fig. 5(b) and in the inset of Fig. 4(a) and 3(a). The consequence of this is that if the  $t \rightarrow \infty$  limit is taken after the  $a \rightarrow 0$  (or  $a \rightarrow a_c$  for  $d = 2$ ) limit, the temperature associated to these ensembles is forever  $T_{QSS} \neq T_{BG}$ . The same feature is revealed if, fixing  $a$ , we analyze the scaling of the crossover time for a large  $N$  (see Fig. 6(a) where we have taken  $a = 0.4$ ). Moreover, the exponent

in the scaling relation  $t_c \sim N^{1.2}$  is very close to what have been found for the QSS of the HMF model:  $t_c \sim N$  [14]. It is also interesting to notice that, for the case we are discussing, this scaling is effective only for large value of  $N$  (say,  $N > 20$ ). For small  $N$  a more intricate, richer behavior appear (see Fig. 6(b)). In particular, for  $N = 5$  we observe for the first time in the case of globally coupled symplectic maps evidence of many-plateau structures (like those in section 2).

## 4 QSS in the Hamiltonian Mean Field model

Along the previous lines of thought we can draw our attention now to a more complex dynamical scenario, that is, Hamiltonian many-body dynamics. In analogy with the globally-coupled symplectic maps of the previous section, we will here focus on *long-range* Hamiltonians. Long-ranged interacting systems constitute nowadays an important subject in many areas of physics, e.g. astrophysics, hydrodynamics, nuclear physics, Bose-Einstein condensates, atomic clusters, plasma physics, and several others [15]. If interaction terms decay as  $r^{-\alpha}$  and  $d$  is the dimension of the system, we say that a classical system has long-range interactions when  $\alpha/d > 1$ . Long range interactions induce long range correlations, and, as a consequence of this, it has been found that these systems show, in a variety of situations, sensible deviations from the BG equilibrium behavior.

In this section we will overview some known aspects and present as well new results for the HMF model [1]. This model has been largely considered in the literature, as it has been found to display a surprisingly rich behavior (see, e.g., [16] for a review). Here we are particularly interested in the appearance, under specific initial conditions (see below), of QSSs that after a certain amount of time cross over to the BG equilibrium. During the QSSs a variety of anomalous behaviors has been detected. Among them, vanishing Lyapunov spectrum, Lévy walks and anomalous diffusion, anomalous distribution of the momenta, non-commutability of the infinite time limit with the thermodynamical limit (see, e.g., [17] and references therein), and, more recently, aging [18,19] and glassy behavior [20]. As some connections have already been established with nonextensive statistical mechanics [17,18,19], these QSSs are candidates for a situation that is correctly described by this formalism.

The HMF Hamiltonian has the following form:

$$H = K + V = \sum_{i=1}^N \frac{p_i^2}{2} + \frac{1}{2N} \sum_{i,j=1}^N [1 - \cos(\theta_i - \theta_j)], \quad (8)$$

where  $\theta_i \in [0, 2\pi)$  is the  $i$ th angle and  $p_i \in \mathbb{R}$  is the conjugate variable repre-

senting the angular momentum (with unit inertial momenta). It is an inertial version of the XY ferromagnetic spin model where the interaction terms couple globally all the spins. Because of the presence of the kinetic part in the Hamiltonian, this model (in opposition with the usual Ising-like spin models) is naturally provided of a dynamics. Also note that it is common use (but not strictly necessary [21]) to divide the potential term by  $N$  in order to make the Hamiltonian (formally) extensive [22].

This system can be analytically solved within the BG canonical formalism, which predicts a second-order phase transition from a low-energy ferromagnetic phase with magnetization  $m \equiv |\mathbf{m}| \neq 0$ , where  $\mathbf{m} \equiv \sum_{i=1}^N \mathbf{m}_i/N$  (with  $\mathbf{m}_i = (\cos \theta_i, \sin \theta_i)$ ), to a high-energy phase with all spins uniformly distributed on the interval  $[0, 2\pi)$  (and consequently  $m = 0$ ). The critical point is at specific energy  $u = u_c \equiv 0.75$ , and the complete equilibrium caloric curve  $T_{BG}(u)$  can be exactly obtained [16]. On the other hand, it is possible to numerically integrate the Hamilton equations at fixed total energy, therefore allowing an analysis in the microcanonical setup. Results show nonequivalence between the two approaches for a range of energy densities below the critical point and for a certain class of initial conditions (which includes the so-called “water bag” initial conditions, characterized by a random distribution of the angular momenta around zero). Numerical simulations show in fact a first regime where the system stays in a non-equilibrium metastable state. It is possible to distinguish this QSS by observing the evolution of the dynamical temperature, here defined in the standard way  $T(t) \equiv 2K(t)/N$  since the total angular momentum is zero. After a short transient the system evolves into a first stage with a temperature  $T_{QSS} < T_{BG}$  and it is only at longer times that it relaxes to the predicted equilibrium value. Very similarly to the case discussed in the previous section, the duration of the QSS diverges linearly as  $N$  goes to infinity [14].

Inside this framework, we present numerical results using a textbook construction (due to Gibbs in fact) of the canonical ensemble as a subsystem of the microcanonical one. It is a purely dynamical approach, in contrast to the analytical derivation mentioned above. We consider in fact a subset of  $M$  spins of the total  $N$  spins in the isolated (microcanonical) system, and study the temperature evolution of this subset, particularly during the metastable state. Temperature is defined as  $T_M(t) \equiv 2K_M(t)/M$ , where  $K_M$  is the kinetic energy of the  $M$  spins. Different criteria may be used in order to choose the  $M$  subsystem. We show two examples, namely selecting the highest and the lowest temperature subsystem. Result are illustrated in Fig. 7 for  $u = 0.69$  [5]: Two curves coming from above and below, respectively. In both cases  $T_M$  is seen to relax after some time to  $T_N$ , *within the metastable state*. Afterwards, both temperatures evolve sharing the same value and perform together the crossover to the predicted  $T_{BG}$ . This result is repeated for two system sizes,  $M = 100$  (solid line) and  $M = 500$  (dashed line), yielding the same behav-

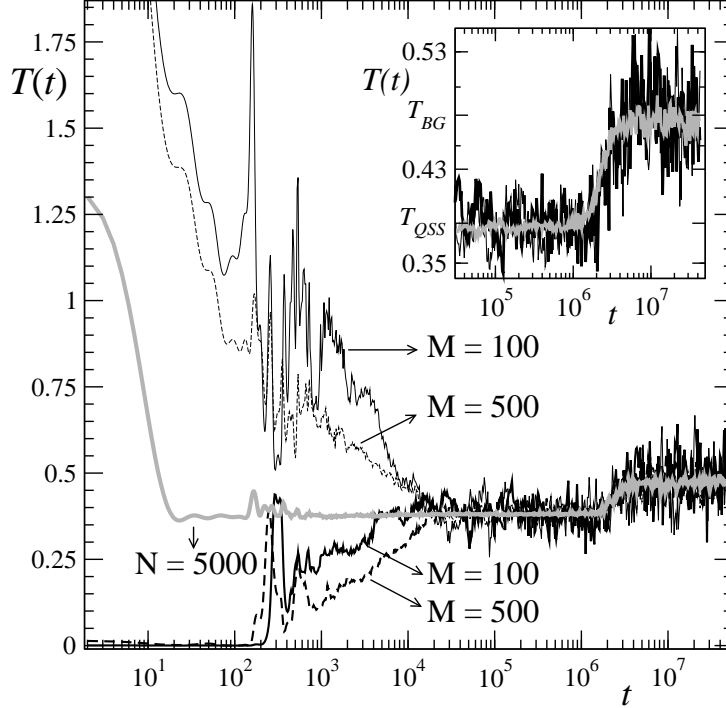


Fig. 7. Temperature evolution of an isolated  $N = 5000$  spin system (Eq. (8)) for  $u = 0.69$  in grey line. We start with “water bag” initial conditions for the momenta (an “almost uniform” distribution inside the range  $-2 \lesssim p_i \lesssim 2$ ; See [5] for details) and magnetization  $m = 1$  ( $\theta_i = 0 \forall i$ ). *Hot* (starting from above) and *cold* (starting from below) smaller subsystems are shown, both with  $M = 100$  (solid thin line) and 500 (dashed thick line). Inset: Magnification of the crossover between  $T_{QSS} \simeq 0.38$  and  $T_{BG} \simeq 0.467$ .

ior. It is important to stress that in the case of the hot subsystems, during the relaxation to  $T_{QSS}$  the temperature value  $T_{BG}$  is crossed with no signs of relaxation to it. Simulations are made using the 4th order symplectic Neri-Yoshida integrator [23] with energy conservation  $\Delta U/U \simeq 10^{-4}$ , and “water bag” initial condition. This result gives a first step into the study of thermal meta-equilibrium of two systems, i.e., the zeroth principle of thermodynamics for the QSS and, furthermore, allows for the possibility of a generalized canonical treatment of the metastable state, which constitutes in fact an ongoing study [24].

We also present a new analysis of how the PDF of the momenta of the  $M$ -subset evolves with time. Results are given in Fig.8. We observe that the PDF for the  $M$ -subset essentially coincides with that of the total  $N$ -system. After a transient of order  $t \sim 10^3$ , the PDF stabilizes into a non-Maxwellian distribution that lasts up to the crossover time  $t \sim 10^6$ . During this whole metastable stage the PDF is well fitted by a  $q$ -Maxwellian with a cut-off,

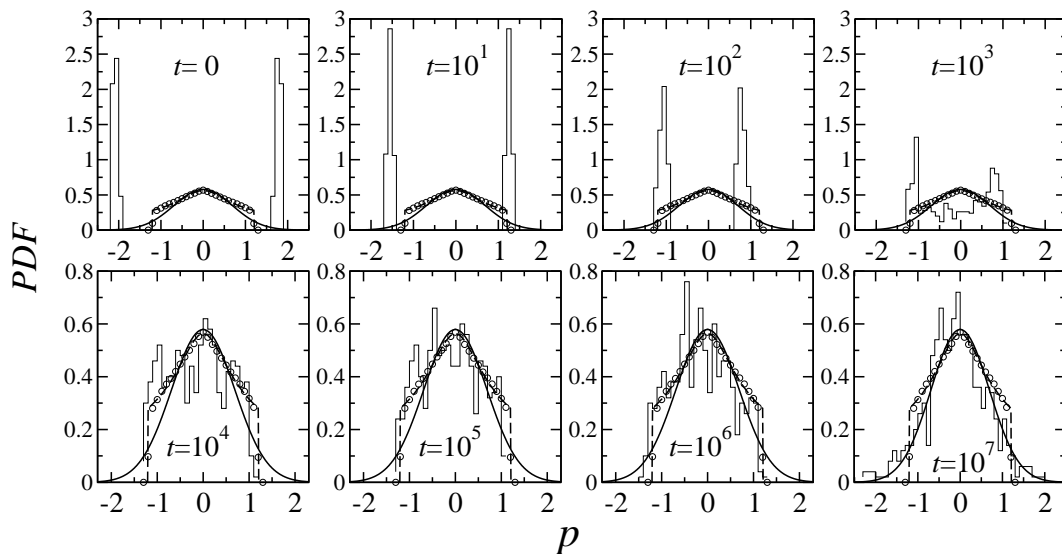


Fig. 8. Snapshots of the evolution of PDF for momenta in the  $\mu$ -space, starting with a “hot water bag” (corresponding to dashed thin curve in Fig. 7). The staired histogram shows the instantaneous PDF at time  $t = 0$  and  $t = 10^k$  (with  $k = 1, 2, \dots, 7$ ), for  $M = 500$  spins inside an  $N = 5000$  spin system. In empty circles, the average of  $10^3$  realizations for  $N = 10^5$  spins (all averages made during the QSS plateau). In dashed line, the  $q$ -exponential fitting curve with  $T = T_{QSS} = 0.38$  and  $q = 3.7$ . Finally, the curve in solid line shows the analytical Gaussian PDF. These last three curves are the same in every frame, and are plotted for reference.

with temperature  $T = T_{QSS}$  and  $q \simeq 3.7$ . The value of  $q$  that we find is different from that calculated in [14]. This may be due to the fact that we are using slightly different (more ordered) initial conditions or to finite-size effects. Our present conjecture is that not only the value of  $q$  can change when the thermodynamic limit is adequately approached (first  $N \rightarrow \infty$ , then  $M \rightarrow \infty$ , and finally  $t \rightarrow \infty$ ), but also the location of the cut-off (in momenta) may go further away, towards infinity. After the crossover time the PDF leaves the QSS anomalous distribution and relaxes to the equilibrium quasi-Maxwellian with  $T = T_{BG}$  (strictly Maxwellian, with no cutoff at all, only for  $N \rightarrow \infty$ ).

## 5 Summary and discussion

Let us summarize our results. We have reviewed and analyzed three quite different dynamical systems: First, the logistic map at the edge of chaos with additive noise, secondly a system composed of globally coupled standard maps, and finally the HMF model. In all three cases a common dynamical feature is found: The occurrence, for certain classes of initial conditions, of metastable states that after a certain time evolve into the stable equilibrium state. These

metastable or quasistationary states appear to be intimately associated to a partial, non-trivial, occupation of phase space, typically (multi)fractal (scale-free and perhaps network-like). This feature retains the system in a non-ergodic state (while held in reserve from entering into all regions of the phase space available to the system). A detailed description for this situation can be given for the simpler case of the logistic map with additive noise at the onset of chaos, i.e., the interplay between a multifractal attractor and a multifractal repeller. This circumstance can also be recognized in the more complex system of two coupled standard maps, since our calculations clearly show the occurrence of quasistationary states and their crossover to final standard chaotic behavior. As we have seen too, the characteristic two-plateau feature is maintained for the case of hundreds of coupled standard maps, and so, we may propose the hypothesis that a fractal occupation holds even for a many-dimensional phase space. The similarities observed between globally coupled symplectic maps and the HMF model indicate that the same state of affairs possibly holds in the case of the QSS detected in the HMF model, a system for which a direct analysis of the  $\Gamma$ -space is much harder.

The importance of these results is underscored by the fact that the QSSs do become permanent when conventional limits are taken in a specific order, e.g. the thermodynamic limit before the infinite time limit in the HMF model. There is a nonuniform convergence feature in the dynamical evolution that leads to an atypical stationary state. Non-commutability of limits occurs too in the case of the maps. For the coupled standard maps this is appreciated when the thermodynamic limit is replaced (for fixed  $a$ ) by the limit of infinite number of coupled maps, or when the chaoticity parameter  $a$  tends (for fixed  $N$ ) towards a specific value ( $a = 0$  for  $d > 2$ , and  $a_c$  if  $d = 2$ ); while in the case of the logistic map it is the limit of vanishing noise that plays an analogous role. Several other common features are found for the QSSs occurring in these different systems. For instance, *in all of them the whole Lyapunov spectrum vanishes*, which seems to pinpoint the cause of the observed anomalies. Also, aging and other glassy properties are both present in the logistic map with additive noise and in the HMF model. These common features suggest a deeper, basic, connection among these systems. As we have seen, the usual BG statistical theory appears to be inadequate in explaining the metastable states, and that a generalization of the usual BG statistics is required. In this respect, the nonextensive theory [6] comes out as the strongest candidate to meet this test.

## Acknowledgments

We acknowledge C. Anteneodo and A. Rapisarda for useful discussions and comments. FB, LGM and CT have benefitted from partial support by FAPERJ,

CNPq and PRONEX (Brazilian agencies). APM was partially supported by SECYT-UNC (Argentinean agency). AR was partially supported by CONA-CyT and DGAPA-UNAM (Mexican agencies).

## References

- [1] M. Antoni and S. Ruffo, Phys. Rev. E **52**, 2361 (1995).
- [2] F. Baldovin, E. Brigatti and C. Tsallis, Phys. Lett. A (2003) in press, cond-mat/0302559.
- [3] A. Robledo, cond-mat/0307285.
- [4] C. Tsallis, J. Stat. Phys. **52**, 479 (1988). For a recent review see M. Gell-Mann and C. Tsallis, eds., *Nonextensive Entropy – Interdisciplinary Applications*, (Oxford University Press, New York, 2004). For full bibliography see <http://tsallis.cat.cbpf.br/biblio.htm>
- [5] L.G. Moyano, F. Baldovin and C. Tsallis, cond-mat/0306374.
- [6] P. Grassberger and M. Scheunert, J. Stat. Phys. **26**, 697 (1981); T. Schneider, A. Politi and D. Wurtz, Z. Phys. B **66**, 469 (1987); G. Anania and A. Politi, Europhys. Lett. **7**, 119 (1988); H. Hata, T. Horita and H. Mori, Progr. Theor. Phys. **82**, 897 (1989); C. Tsallis, A.R. Plastino and W.-M. Zheng, Chaos, Solitons and Fractals **8**, 885 (1997).
- [7] F. Baldovin and A. Robledo, Phys. Rev. E **66**, 045104(R) (2002); F. Baldovin and A. Robledo, cond-mat/0304410.
- [8] P.G. De Benedetti and F.H. Stillinger, Nature **410**, 267 (2001).
- [9] J.P. Bouchaud, L.F. Cugliandolo, J. Kurchan and M. Mezard, in *Spin Glasses and Random Fields*, A.P. Young, editor (World Scientific, Singapore, 1998).
- [10] E. Ott, *Chaos in dynamical systems* (Cambridge University Press, Cambridge, 1993).
- [11] G.M. Zaslavsky, R.Z. Sagdeev, D.A. Usikov and A.A. Chernikov, *Weak chaos and quasi-regular patterns* (Cambridge University Press, Cambridge, 1991).
- [12] R. Livi, M. Pettini, S. Ruffo and A. Vulpiani, J. Stat. Phys. **48**, 539 (1987).
- [13] R.S. Mackay, J.D. Meiss and I.C. Percival, Physica D **13**, 55 (1984).
- [14] V. Latora, A. Rapisarda and C. Tsallis, Phys. Rev. E **64**, 056134 (2001).
- [15] See, for example, T. Dauxois, S. Ruffo, E. Arimondo and M. Wilkens Lecture Notes in Physics **602**, 140 (Springer, Berlin, 2002).



- [16] T. Dauxois, V. Latora, A. Rapisarda and S. Ruffo in *Dynamics and Thermodynamics of Systems with Long-Range Interactions*, eds T. Dauxois, S. Ruffo, E. Arimondo and M. Wilkens Lecture Notes in Physics **602**, 140 (Springer, Berlin, 2002).
- [17] C. Tsallis, A. Rapisarda, V. Latora and F. Baldovin, in *Dynamics and Thermodynamics of Systems with Long-Range Interactions*, eds T. Dauxois, S. Ruffo, E. Arimondo and M. Wilkens Lecture Notes in Physics **602**, 140 (Springer, Berlin, 2002).
- [18] M.A. Montemurro, F. Tamarit and C. Anteneodo, Phys. Rev. E **67**, 031106 (2003).
- [19] A. Pluchino, V. Latora and A. Rapisarda, Physica D (2004) in press, cond-mat/0303081.
- [20] A. Pluchino, V. Latora and A. Rapisarda, cond-mat/0306374.
- [21] C. Anteneodo and C. Tsallis, Phys. Rev. Lett. **80**, 5313 (1998); C. Anteneodo, cond-mat/0311084.
- [22] M. Kac, G. Uhlenbeck and P.C. Hemmer, J. Math. Phys. **4**, 216 (1963).
- [23] F. Neri, *Lie algebras and canonical integration*, Department of Physics, University of Maryland, preprint (1988); H. Yoshida, Phys. Lett. A **150**, 262 (1990).
- [24] F. Baldovin, L.G. Moyano and C. Tsallis, in progress.